Oncogene (2019) 38:5227–5238
https://doi.org/10.1038/s41388-019-0788-4

ARTICLE

piRNA-823 delivered by multiple myeloma-derived extracellular vesicles promoted tumorigenesis through re-educating endothelial cells in the tumor environment

Beibei Li[1] · Jiaxin Hong[1,2] · Mei Hong[1,3] · Yajun Wang[1] · Tingting Yu[1] · Sibin Zang[1] · Qiuling Wu[1]

Received: 6 June 2018 / Revised: 5 March 2019 / Accepted: 6 March 2019 / Published online: 19 March 2019

Abstract

Extracellular vesicles (EVs) can carry a wide array of RNAs in the tumor microenvironment, and are crucial for communication between tumor and surrounding stromal cells, including endothelial cells. Piwi-interacting RNAs (piRNAs) are important regulators implicated in the pathogenesis of multiple myeloma (MM). However, little is understood about the role of piRNA-823 in intercellular communication between MM and endothelial cells. In this study, we found that piRNA-823 mainly accumulated in EVs from peripheral blood of MM patients and EVs derived from MM cells (MM-derived-EVs). Increased piRNA-823 expression was associated with late stages and poor prognosis of MM. The MM-derived-EVs effectively transferred piRNA-823 to EA.hy926 endothelial cells. The piRNA-823 mimic and inhibitor were designed to upregulate or to suppress the endogenous function of piRNA-823. Transfection with piRNA-823 mimic or treatment with MM-derived-EVs significantly promoted the proliferation, tube formation, and invasion of EA.hy926 cells by enhancing the expression of VEGF, IL-6, and ICAM-1 and attenuating apoptosis. EA.hy926 cells transfected with piRNA-823 mimic or pre-treated with MM-derived-EVs promoted the growth of xenograft MM in mice. In contrast, the transfection with piRNA-823 inhibitor or treatment with EVs from piRNA-823 inhibitor-transfected-MM cells had diametrically opposite effects. Our findings demonstrated that piRNA-823 carried by MM-derived-EVs is essential for the re-education of ECs toward a unique environment amenable to the growth of MM cells by altering its biological characteristics. Our findings may pave the way for the development of new piRNA-mediated prognostic stratification and therapeutic strategies for MM.

Introduction

Multiple Myeloma (MM) is characterized by an abnormal clonal expansion of plasma cells in the bone marrow (BM), which leads to accumulation of monoclonal proteins in the blood, urine, and end-organ damage [1, 2]. MM cells can circulate and spread into end-organs, resulting in poor prognosis. Cells, including mesenchymal stem cells, endothelial cells, and fibroblasts in the tumor microenvironment, play an important role in the spread of tumor cells. Understanding the molecular mechanisms underlying the interaction between MM cells with tumor microenvironmental cells is crucial for the development of new therapeutic strategies for MM.

In the development of MM, endothelial cells (ECs) in tumor microenvironments are essential for the growth, survival, and spread of MM cells [3, 4]. Tumor-associated endothelial cells are biologically unique. They proliferate fast and are highly sensitive to growth factors, resistant to apoptotic stimuli and strongly pro-angiogenic, and thereby are instrumental in the tumor growth [5, 6]. Previous studies had shown that ECs of malignant origin, such as B-cell lymphomas, glioblastoma, and neuroblastoma, are cytogenetically abnormal, with chromosomal nonreciprocal translocations, chromosomal deletion, and marker

These authors contributed equally: Beibei Li, Jiaxin Hong, Mei Hong

Supplementary information The online version of this article (https://doi.org/10.1038/s41388-019-0788-4) contains supplementary material, which is available to authorized users.

✉ Qiuling Wu
wuqiuling927@qq.com

[1] Institute of Hematology, Union Hospital, Tongji Medical College, Huazhong University of Science and Technology, Wuhan, China

[2] Cancer Center, Union Hospital, Tongji Medical College, Huazhong University of Science and Technology, Wuhan, China

[3] Collaborative Innovation Center of Hematology, Soochow University, Suzhou, China

chromosome [6–11]. A study reported that neoplastic circulating ECs had 13q14 deletion in the MM patients [12]. Furthermore, recent studies indicated that myeloma ECs might not be congenitally abnormal and instead, passively re-educated by MM cells. However, so far, how the MM cells educate normal ECs into tumorigenesis is poorly understood.

Extracellular vesicles (EVs), the lipid bilayer spheres ranging from 40 to 1000 nm in diameter, are released from most cells lines and contain various functional proteins, mRNAs, and miRNAs [13, 14]. EVs can be internalized into target cells and thus regulate their biological functions by activating key signaling pathways [15]. EVs are crucial for the cross-talk between cancer and surrounding cells in the tumor microenvironment and play a pivotal role in the development and progression of cancer [16, 17]. EVs released by chronic lymphocytic leukemic cells reprogram mesenchymal stem cells to adopt a cancer-associated fibroblast phenotype with enhanced proliferation, migration, and secretion of cytokines, which can further favor the tumor cell growth [18]. EVs were detected in the supernatants of cultured MM cells [19]. Under chronic hypoxia, exosomes secreted by MM cells enhance angiogenesis by targeting factor-inhibiting hypoxia-inducible factor-1 via miR-135b [17]. However, how EVs derived from MM cells (MM-derived-EVs) functionally modulate ECs in the tumor environment has not been clarified clearly.

Piwi-interacting RNAs (piRNAs) are a class of small non-coding RNAs containing 26–31 nucleotides in length [20–22]. Previous studies have demonstrated that piRNAs could interact with PIWI protein to epigenetically and post-transcriptionally silence transposable elements in germline stem cells [23–26]. Furthermore, piRNAs are associated with the development and progression of several types of cancers [27–29]. Our previous study has found that piRNA-823 was implicated in the pathogenesis of MM, and piRNA-823 silencing in MM cells reduced the vascular endothelial growth factor (VEGF) production and its pro-angiogenic activity [30]. However, whether piRNA-823 can be delivered by MM cells to ECs and how the EVs-educated ECs impact the growth of MM tumors remains elusive.

This study aimed to examine the expression of piRNA-823 in the peripheral blood EVs of MM patients and determine its potential value in prognostic stratification. We further studied the role of piRNA-823 in possible intercellular communications between MM cells and ECs through MM-derived-EVs. Our data demonstrated that MM-derived-EVs could enhance the survival and pro-angiogenic activity of ECs by delivering piRNA-823, thereby creating a favorable microenvironment for MM.

Results

High levels of piRNA-823 in peripheral blood EVs from MM patients

Our previous study showed that piRNA-823 in biopsied bone marrow specimens of newly diagnosed MM patients was significantly higher than the healthy controls [30]. We successfully isolated the EVs from peripheral blood or the supernatant of cultured MM cells (Supplementary Fig.1). To sought the implications of piRNA-823 in the diagnosis and prognosis, we determined the relative levels of piRNA-823 in EVs of 36 MM patients and healthy controls using qRT-PCR. A total of 28 out of 36 EV samples contained piRNA-823, and the relative levels of piRNA-823 in the EVs were significantly higher than in plasma (Supplementary Fig.2), suggesting that the blood piRNA-823 levels are predominantly associated with EVs. However, the piRNA-823 level in EVs was not associated with gender, age, and isotype, but it was positively associated with the disease stages ($r = 0.98$, $P < 0.01$, Fig. 1a). piRNA-823 was found to be significantly increased in peripheral EVs of the patients with stage II and III MM. Further analysis indicated that increased piRNA-823 in peripheral EVs was positively correlated with higher levels of β2-MG ($r = 0.800$, $P < 0.01$), serum Cr ($r = 0.468$, $P < 0.01$), and lower levels of Hb ($r = -0.393$, $P < 0.05$), but negatively correlated with blood calcium ($r = -0.019$, $P > 0.05$) and LDH ($r = 0.138$, $P > 0.05$). These findings showed that high levels of piRNA-823 in peripheral EVs were associated with advanced stage of MM and had the potential to serve as a biomarker for stages and prognosis of MM.

Also, we cultured $CD138^+$ cells from the bone marrow of MM patients and found that the levels of piRNA-823 in the EVs purified from the supernatant of the same amount of cultured $CD138^+$ cells were significantly higher than that in their parental cells (Fig. 1b). Similarly, in Fig. 1c, EVs were purified from the culture supernatant of the same amount of parental MM cell lines. Higher levels of piRNA-823 were detected in EVs from three types of cultured MM cells compared to their parental MM cells. These results indicate that MM cells produced EVs encapsulating a large amount of piRNA-823.

MM-derived-EVs effectively transport piRNA-823 to ECs

To test the function of EVs, they were purified from RPMI 8226 cells that had been labeled with CFSE and transfected with Cy3-labeled piRNA-823. The transfection efficiency of Cy3-labeled piRNA-823 in RPMI 8226 is shown in Supplementary Fig.3. Subsequently, ECs were treated with the EVs

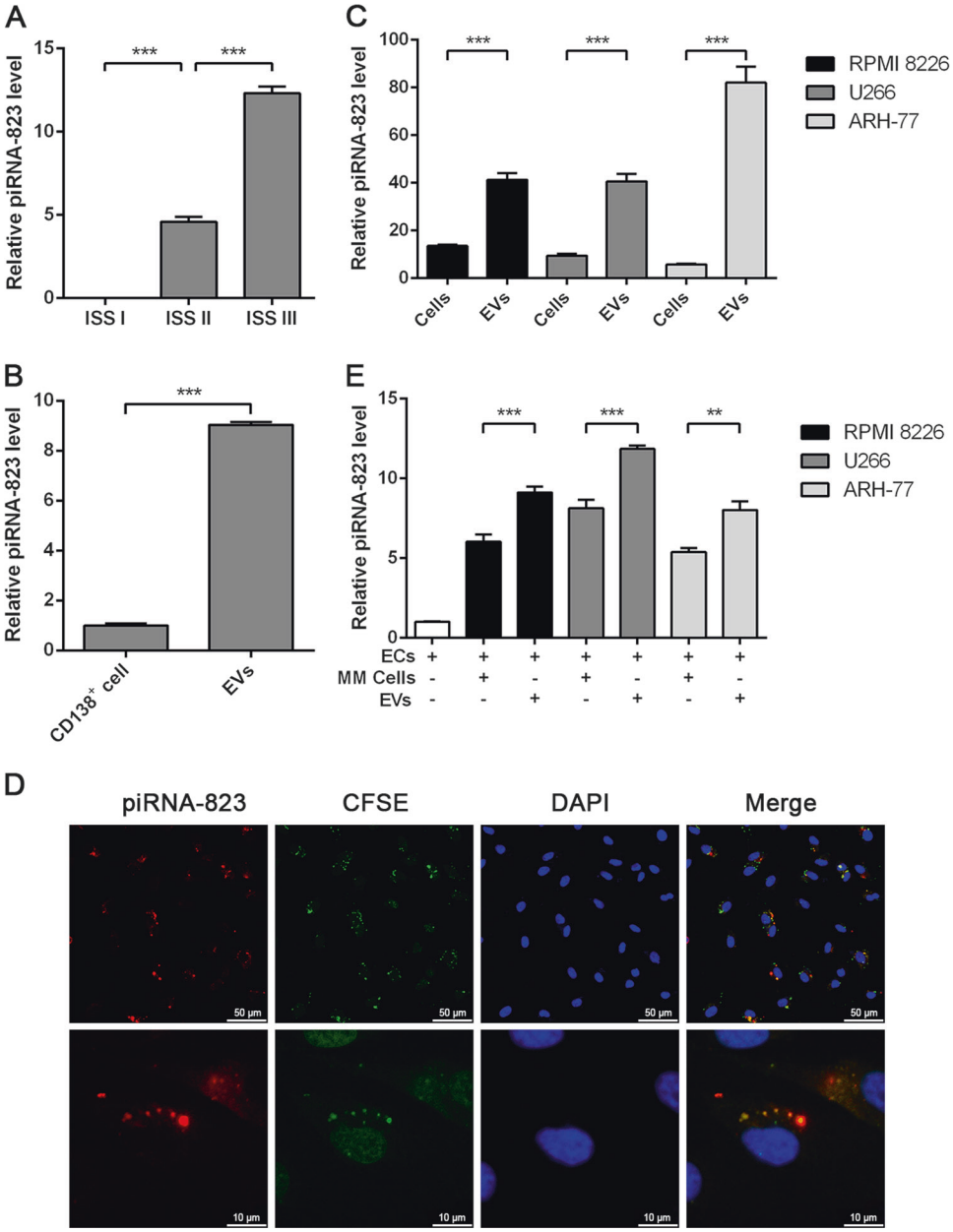

Fig. 1 piRNA-823 was accumulated in MM-derived-EVs, and MM-derived-EVs effectively transferred piRNA-823 to EA.hy926 cells. **a** piRNA-823 levels in EVs from peripheral blood of MM patients at different stages. ISS I ($n = 6$), ISS II ($n = 11$), ISS III ($n = 19$). **b** piRNA-823 levels in bone marrow $CD138^+$ cells of MM patients and EVs derived from the same amount of cultured $CD138^+$ cells. **c** piRNA-823 levels in MM cell lines (RPMI 8226, U266, ARH-77 cells), and EVs derived from the same amount of parental MM cell lines. **d** Representative confocal microscopy images of the fusion of ECs with MM-derived-EVs. EA.hy926 cells were cultured with CFSE labeled EVs (green) derived from RPMI 8226 cells which were pre-transfected with Cy3-piRNA-823 (red). Nuclear counter-staining was performed using DAPI (blue). **e** piRNA-823 levels in EA.hy926 cells treated with MM cell lines RPMI 8226, U266, ARH-77 cells or their EVs. Values are expressed as means ± SEM of three independent experiments. $^{**}P < 0.01$, $^{***}P < 0.001$ (color figure online)

for 48 h. The laser confocal imaging indicated that both CFSE and Cy3 fluorescent signals colocalized in recipient ECs (Fig. 1d). After ECs and MM cell lines were co-cultured in the transwell co-culture system for 24 h as described in Materials and methods, the levels of piRNA-823 in ECs were measured by qPCR. The results showed that the relative levels of piRNA-823 in the ECs co-cultured with RPMI 8226, U266, or ARH-77 cells were significantly higher than in the unmanipulated ECs, and piRNA-823 was higher in ECs treated with EVs compared to ECs co-cultured with MM cells (Fig. 1e, $P < 0.01$). These data clearly demonstrate that MM-derived-EVs effectively delivered piRNA-823 into ECs under our experimental conditions.

MM-derived-EVs enhance the proliferation and inhibit the apoptosis of ECs

The treatment based grouping of EA.hy926 cells are described within the Materials and methods section. The transfection efficiency of piRNA-823 mimic in EA.hy926 cells was shown in Supplementary Fig.4. To understand the role of piRNA-823 in the proliferation and survival of ECs, we determined the proliferation and apoptosis-related molecule expression, as well as ROS and NO production of EA.hy926 cells in different groups. The relative ratio of the protein expressions were analyzed by Image J software (Supplementary Fig.5).

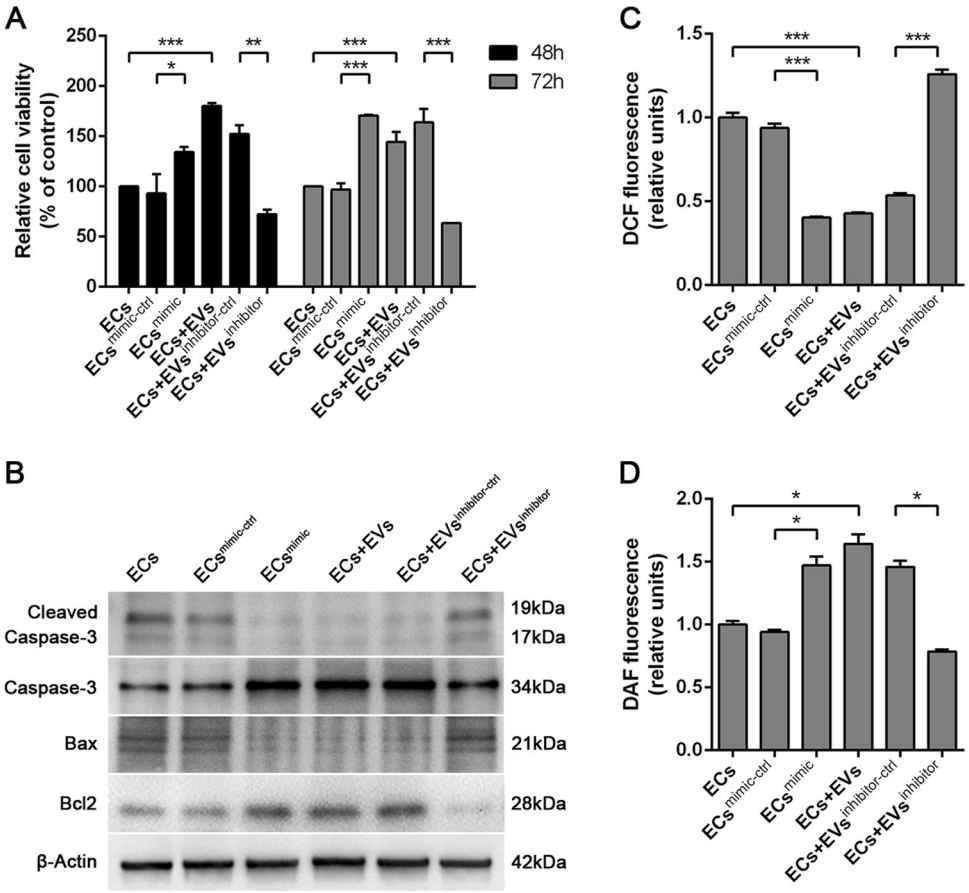

Fig. 2 piRNA-823 transferred by MM-derived-EVs modulates the proliferation, apoptosis and oxidative stress of ECs. The treatment based grouping of EA.hy926 cells are described within the Materials and Methods section. The ECs were treated with or without different EVs for 48 or 72 h. **a** The cell proliferation of different groups of ECs was determined by CCK-8 assays. **b** The relative levels of Caspase-3, Cleaved Caspase-3, Bax and BcL-2 to the control β-actin in different groups of ECs were determined by western blotting. **c**, **d** The levels of intracellular ROS and NO in different groups of ECs were determined by flow cytometry using specific dyes. Data are from representative images or expressed as the mean ± SEM of each group from three separate experiments. $^{*}P < 0.05$, $^{**}P < 0.01$, $^{***}P < 0.001$

In comparison with $ECs^{mimic\text{-}ctrl}$ group, transfection with piRNA-823 mimic in ECs^{mimic} group significantly enhanced the proliferation of ECs, with inhibition of Caspase-3 activation, downregulation of Bax expression, and upregulation of Bcl2 expression (Fig. 2a, b). The transfection with piRNA-823 mimic significantly increased NO production, but decreased the ROS production in ECs (Fig. 2c, d). In ECs + EVs group, the MM-derived-EVs significantly promoted the growth of ECs, with a decrease in Caspase-3 activation and Bax expression, but had an increased Bcl-2 expression. However, the pro-proliferative and anti-apoptotic effect of MM-derived-EVs on ECs could be inhibited by the piRNA-823 inhibitor. In comparison with $EVs^{inhibitor\text{-}ctrl}$-treated ECs in ECs + $EVs^{inhibitor\text{-}ctrl}$ group, the proliferation of $EVs^{inhibitor}$-treated ECs in ECs + $EVs^{inhibitor}$ group was significantly decreased, accompanied by increased apoptosis-related protein and ROS production and decreased NO production in $EVs^{inhibitor}$-treated ECs. Together, these findings show that piRNA-823 delivered by MM-derived-EVs, could promote the proliferation of ECs by regulating apoptosis and production of ROS and NO in vitro.

piRNA-823 transferred by MM-derived-EVs promotes angiogenesis and invasion of ECs

To further investigate the role of piRNA-823 in angiogenesis, we compared the tube formation of different groups of ECs (Fig. 3a). The transfection with piRNA-823 mimic in ECs^{mimic} group significantly enhanced the tube formation in ECs. Similarly, treatment with EVs increased the tube formation of ECs in ECs + EVs group, while the treatment with $EVs^{inhibitor}$ dramatically decreased the tube formation in ECs + $EVs^{inhibitor}$ group compared to the $EVs^{inhibitor\text{-}ctrl}$ treatment in ECs + $EVs^{inhibitor\text{-}ctrl}$ group.

Since the vascular endothelial growth factor (VEGF) and interleukin 6 (IL-6) can promote angiogenesis of ECs, we assessed the levels of VEGF and IL-6 in the supernatants of different groups of cultured ECs. As shown in Fig. 3b, c, the levels of VEGF and IL-6 were significantly higher in the supernatants of cultured ECs^{mimic} than in the ECs and $ECs^{mimic\text{-}ctrl}$ ($P < 0.05$; $P < 0.0001$, respectively). The treatment with MM-derived-EVs in ECs + EVs group significantly increased the secretion of VEGF and IL-6 by ECs compared to the unmanipulated ECs^{ctrl} group. Whereas, the

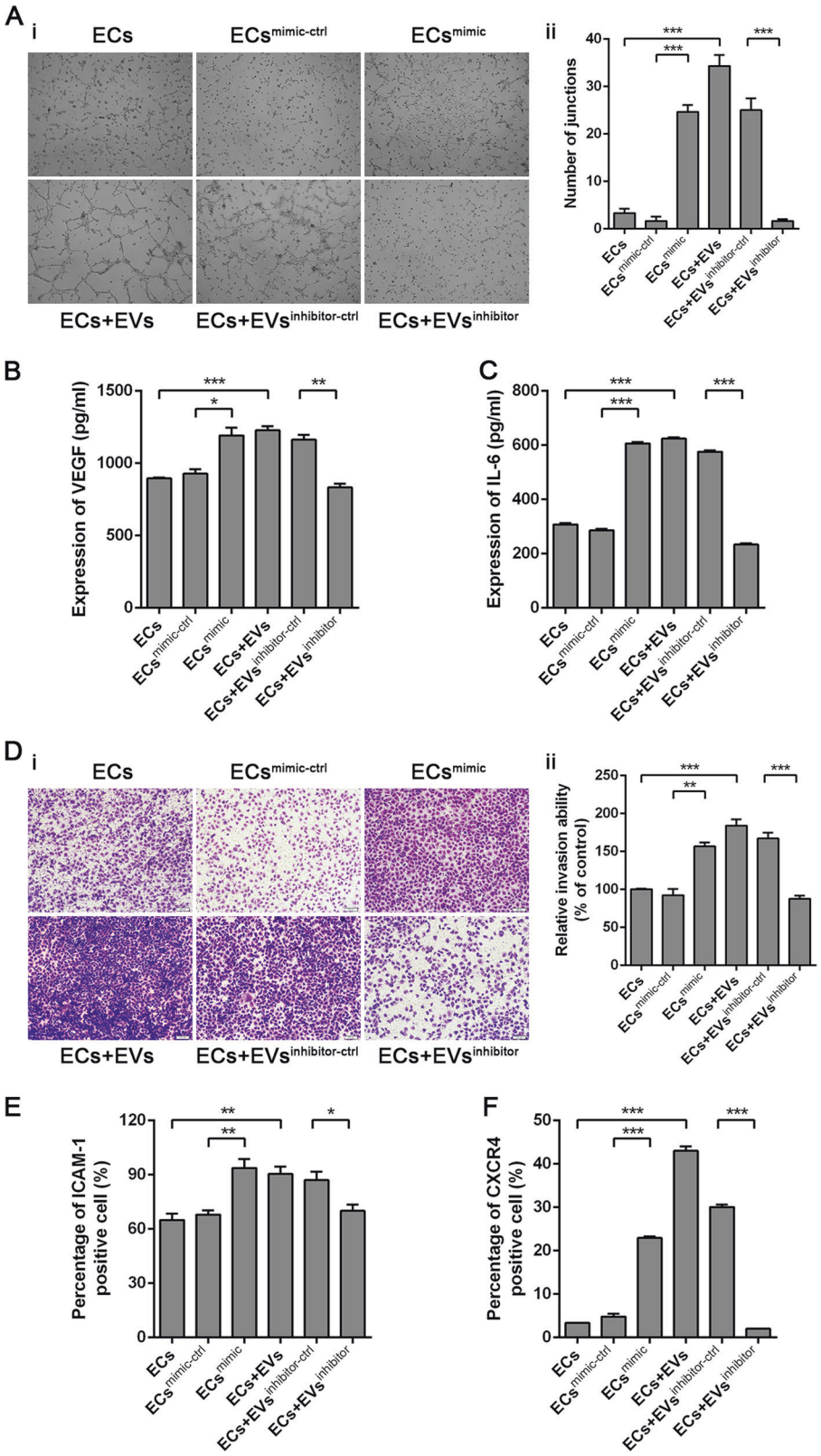

Fig. 3 piRNA-823 transferred by MM-derived-EVs promotes angiogenesis and invasion of ECs. The treatment based grouping of EA.hy926 cells are described within the Materials and Methods section. The ECs were treated with or without different EVs for 24 or 48 h. **a i** EA.hy926 cells were seeded on top of extracellular Matrigel in the presence of conditioned media collected from different groups of ECs. Tube formation was assessed by an inverted light microscope. Photographs are representative of three independent experiments. **ii** Quantitative tube formation assay. The *y*-axis represents the number of cell junctions. **b**, **c** The VEGF and IL-6 levels in the supernatants of different ECs groups were quantified by ELISA. **d i** Cell invasion ability of different ECs groups was evaluated using a 24-transwell chamber with Matrigel. ECs were added to the upper chamber that had been coated with Matrigel and the lower chamber was added with 10% FBS M199 medium. Invasive cells on the bottom surface of the upper chambers were stained by crystal violet and assessed under an inverted light microscope. **ii** Quantitative transwell migration assay. The *y*-axis represents the number of migrating cells. **e**, **f** The percentages of ICAM-1^+ and $CXCR4^+$ cells in different groups of ECs were analyzed by flow cytometry. Data were from representative images or expressed as the mean ± SEM of each group from three independent experiments. $^*P < 0.05$, $^{**}P < 0.01$, $^{***}P < 0.001$

treatment with $EVs^{inhibitor}$ in $ECs + EVs^{inhibitor}$ group significantly decreased the secretion of VEGF and IL-6 by ECs compared to $ECs + EVs^{inhibitor\text{-}ctrl}$ group ($P < 0.01$ or $P < 0.001$). These results showed that piRNA-823 delivered by MM-derived-EVs, promoted the angiogenesis by enhancing VEGF and IL-6 secretion of ECs.

Since aggressive proliferation and enhanced angiogenesis were associated with invasion of tumors, we finally examined the effect of piRNA-823 on the invasion of ECs by transwell invasion assays. The invasion ability of ECs in ECs^{mimic} group or EVs-treated ECs in ECs + EVs group was significantly stronger than in $ECs^{mimic\text{-}ctrl}$ or unmanipulated ECs. As compared with $EVs^{inhibitor\text{-}ctrl}$-treated ECs, $EVs^{inhibitor}$-treated ECs was found to reduce the invasion ability dramatically. ($P < 0.001$, Fig. 3d). Flow cytometry further revealed that the proportion of ICAM-1^+ ECs and $CXCR4^+$ ECs in ECs^{mimic} group or ECs + EVs group were significantly increased compared to $ECs^{mimic\text{-}ctrl}$ or unmanipulated ECs. Whereas, the treatment with $EVs^{inhibitor}$ in $ECs + EVs^{inhibitor}$ group dramatically decreased the percentages of ICAM-1^+ ECs and $CXCR4^+$ ECs compared to $ECs + EVs^{inhibitor\text{-}ctrl}$ group (Fig. 4e, f). These findings showed that piRNA-823, delivered by MM-derived-EVs, promoted the invasion of ECs by inducing ICAM-1 and CXCR4 expression.

piRNA-823 transferred by MM-derived-EVs promotes the growth of xenograft tumors in vivo

ECs were transfected with piRNA-823 mimic or scramble control or pre-treated with EVs, $EVs^{inhibitor\text{-}ctrl}$, or $EVs^{inhibitor}$ for 48 h. Subsequently, NOD/SCID mice were injected subcutaneously with a mixture of different ECs and RPMI 8226 cells at a ratio of 1:10. Post-implantation, the growth, and development of tumors were monitored for 6 weeks. In comparison with ECs, the ECs^{mimic} or EVs-treated ECs conspicuously increased the volume of xenograft tumors (Fig. 4a, b). The tumor mass in mice xenografted with MM cells and $EVs^{inhibitor}$-treated ECs was significantly reduced as compared with $EVs^{inhibitor\text{-}ctrl}$-treated ECs. In accordance with this finding, the immunohistochemical detection showed that, in the excised tumors from mice xenografted with MM cells and ECs^{mimic} or EVs-treated ECs in ECs^{mimic} group or ECs + EVs group, the tumor cell proliferation was enhanced with an increased expression of Ki-67, CD31, and CD34, along with a decrease in Cleaved Caspase-3 and increased angiogenesis. However, the pro-tumorigenic and pro-angiogenic activity of EVs-treated ECs was reduced by piRNA-823 inhibition. Increased Cleaved Caspase-3 expression and decreased Ki-67, CD31, and CD34 expression were found in $ECs + EVs^{inhibitor}$ group as compared with in $ECs + EVs^{inhibitor\text{-}ctrl}$ group (Fig. 4c). We are driven to the conclusion that ECs with a higher level of piRNA-823 might present a survival advantage to MM cells in vivo.

Discussion

In this study, for the first time, we found that the levels of piRNA-823 in peripheral blood EVs were higher in MM patients than in healthy controls. piRNA-823 was significantly increased in the peripheral EVs of patients with stage II and III MM or the patients with renal injury and hyphemia, suggesting that piRNA-823 might serve as a potential indicator for the prognosis and stratification of MM. Moreover, our results showed piRNA-823 was concentrated in MM-derived-EVs. piRNA-823 could be delivered to ECs via MM-derived-EVs to promote the proliferation, angiogenesis, invasion of ECs which could in turn promote the MM cell proliferation and eventually lead to the development and progression of MM. In general, our findings demonstrate that piRNA-823 carried by MM-derived-EVs are essential for the re-education of ECs toward a unique environment amenable to the growth of MM cells by altering its biological features.

The circulating miRNAs have been recently recognized as an appealing non-invasive biomarker in the diagnosis and prognosis of many cancers including MM because they have tumor-specific expression profiles and are highly stable in blood. Nonetheless, some circulating miRNAs are subject to hemolysis, even at low hemolytic levels. EVs were found to protect miRNAs from the impact of the surrounding environment. EVs can concentrate miRNAs, which is instrumental to diagnosis. Moreover, miRNAs in EVs are more actively secreted by cancer cells as compared to the circulating miRNAs, which are passively released from apoptotic and necrotic cells. Therefore, the miRNAs within circulating EVs might be indicative of their tumor origin and represent the actual level of tumor burden in cancer patients [31, 32]. Manier et al. analyzed exosomes isolated from serum samples of 156 myeloma patients using a qRT-PCR array for 22 miRNA found only two miRNAs (let-7b and miR-18a) could serve as independent predictors for progression-free survival (PFS) and overall survival (OS) [33]. Herein, we for the first time, demonstrated that elevated level of piRNA-823 encapsulated in peripheral blood EVs bore an obvious positive correlation with advanced clinical stages and poor clinical prognosis of MM. Our findings suggested that circulating piRNA-823 in EVs might serve as a novel marker for diagnostic and prognostic stratification of MM.

It is known that myeloma endothelial cells are different genetically and functionally compared to their normal counterparts [12]. However, no evidence could indicate that these genetic abnormalities are due to gene mutation or active

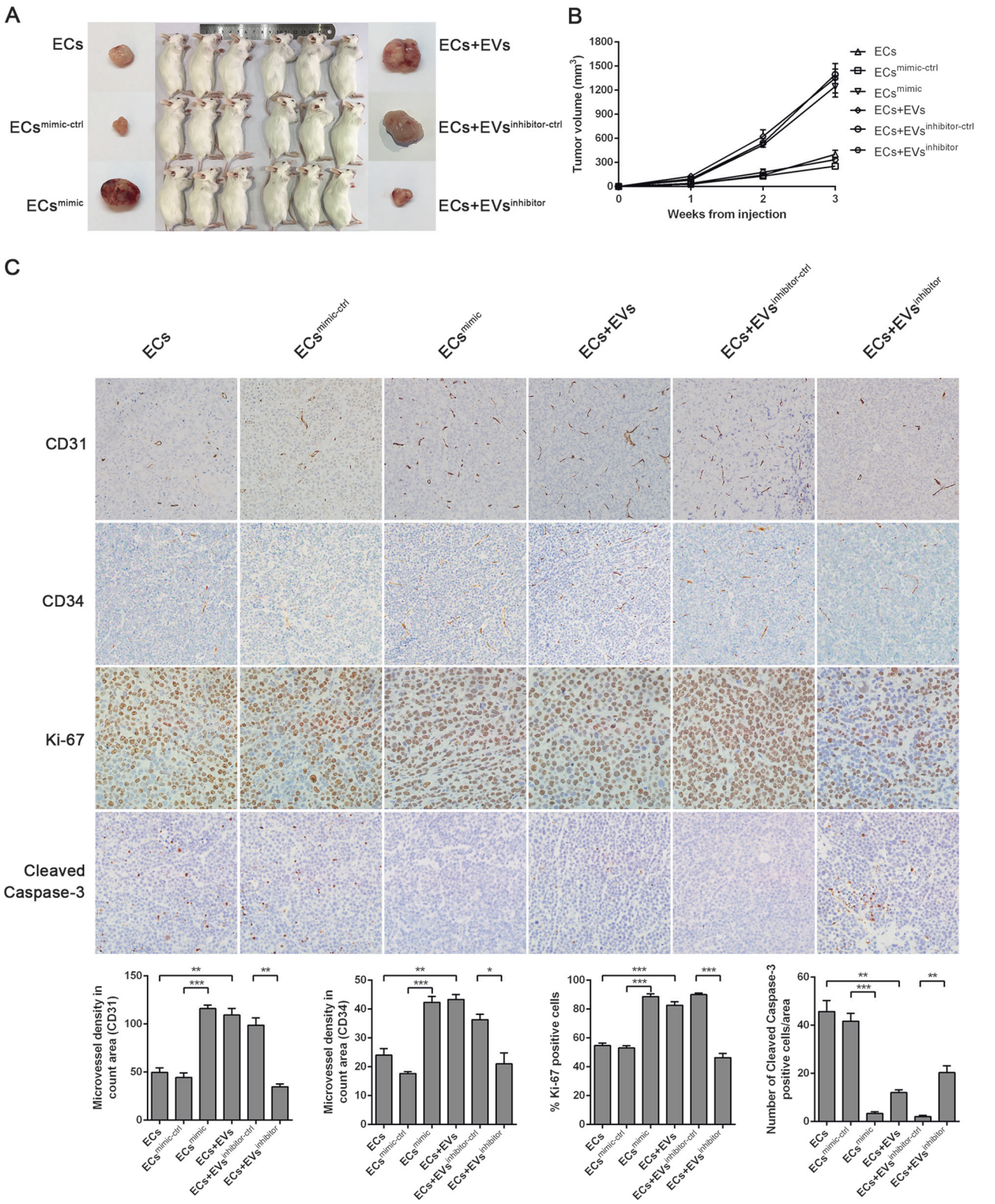

Fig. 4 piRNA-823 transferred by MM-derived-EVs promotes the growth of xenograft MM tumors in mice by enhancing angiogenesis and inhibiting apoptosis. Individual NOD/SCID mice were implanted subcutaneously with 5×10^6 PRMI 8226 cells mixed with 5×10^5 EA. hy926 cells from different groups, and the development and growth of tumors were monitored up to 6 weeks post-implantation. **a**, **b** Tumor size was measured, and the tumor growth curves were plotted. **c** Representative immunohistochemical staining of CD31, CD34, Ki-67, Cleaved Caspase-3 in tumor xenografts are shown. Data were expressed as the mean ± SEM of each group from three microscopic fields. $^*P < 0.05$, $^{**}P < 0.01$, $^{***}P < 0.001$

regulation by tumor cells. ECs can take up EVs shed from many types of cells including monocytes, activated platelets, and tumor cells [34–37]. Glioblastoma-derived-EVs and pancreatic cancer-derived-exosomes reportedly express angiogenic proteins, mRNAs and miRNAs that activate angiogenesis-related gene expression in ECs [38, 39]. Besides, the mounting evidence demonstrated that tumor-derived-EVs enhanced the proliferation and angiogenesis of ECs in chronic myelogenous leukaemia [40, 41]. Our study found that MM-derived-EVs promoted the proliferation, migration, and capillary structure formation of ECs and enhanced their secretion of VEGF, IL-6, ICAM-1, and CXCR4, which indicated the malignant transformation of endothelial cells. Additionally, ECs pulsed with MM-derived-EVs were strongly protumoral, promoting myeloma cell growth and survival both in vitro and in vivo. These findings strongly indicate that MM cells secreted EVs to actively create a new tumor microenvironment, which in turn promotes the tumor proliferation, survival, angiogenesis, and metastasis.

EVs have been proved to contain a wide array of miRNA, but it is still unknown which one is preferentially secreted by MM cells to target bone marrow stromal cells. The miR-92a and miR-210 were found to be enclosed in leukemia-derived-exosomes, to enhance endothelial cell migration and tube formation after being transferred into ECs [36, 37]. Exosomal miR-135b shed from hypoxic MM cells enhanced angiogenesis by suppressing its target factor-inhibiting hypoxia-inducible factor-1 (FIH-1) in ECs [17]. piRNA is a kind of small RNAs, which is not expressed in the normal somatic cells but expressed only in germ cells and tumor cells, so it possesses an excellent tumor specificity. Our previous study showed that mesenchymal stem cells from older mice express higher levels of PIWI protein PiwiL2 than young mice [42]. Moreover, mice would progress to myelodysplastic syndromes or leukemia when DICER area containing PIWI domain was selectively silenced in mesenchymal osteoprogenitors [43]. These studies demonstrated that piRNA might be capable of inducing malignant transformation of bone marrow stromal cells. In this study, for the first time, we reported that upregulation of piRNA-823 in ECs could significantly promote the proliferation, angiogenesis, and invasion of ECs, which strongly suggests that piRNA-823 plays a pivotal role in the malignant transformation of endothelial cells. Furthermore, we found piRNA-823 was highly expressed in MM-derived-EVs, and the downregulation of piRNA-823 in EVs could significantly decrease malignant transformation of EVs-treated-ECs. Our data strongly suggest that piRNA-823 is a crucial element encapsulated in MM-derived-EVs and can help to establish a favorable endothelial microenvironment that ultimately promotes MM progression.

So far, no studies have positively shown whether miRNA could be stable in EV structure. piRNAs are a novel class of non-coding single strand RNAs that specifically interact with the PIWI proteins essential to the biogenesis, function, and stabilization of piRNA [23]. Recent researches found PIWI-family protein was one of the few proteins, which can protect miRNAs from degradation. MicroRNAs in cell secreting EVs were bound with Ago2 complexes, which protect miRNAs from degradation by RNases [44]. It has been well established that Piwi-family proteins can increase the stability of miRNAs [45, 46]. Compared with microRNA, piRNAs are more stable and abundant in peripheral EVs due to the protection of PIWI proteins. In this study, we demonstrated that piRNA-823 had long-term stability in EVs derived from peripheral blood and cultured MM cell supernatant. Furthermore, 6-week observation on xenograft murine models showed that the effect of piRNA-823 on subcutaneous xenotransplanted MM models was certainly effective and lasting. Our study highlights a new dimension in the piRNA-mediated therapeutics for MM.

In summary, our study revealed how MM cells re-educated ECs in the tumor environment via MM-derived-EVs. More importantly, we found that piRNA-823 is the key regulator that is highly expressed in MM-derived-EVs in a stable manner and could promote the malignant transformation of ECs. Our research provides the rationale for the development of new piRNA-mediated prognostic stratification and therapeutic strategy for MM. However, the signaling pathways by which piRNA-823 in MM-derived-EVs modulates the genetic and epigenetic changes of ECs are warranted.

Materials and methods

Patients and clinical samples

The study protocol was approved by the Institutional Review Board of Wuhan Union Hospital, Huazhong University of Science and Technology, and all study participants provided written informed consent. A total of 36 MM patients diagnosed in our hospital were enrolled from November 2014 to April 2016. All of the patients had not received any specific anti-MM therapy before enrollment.

Peripheral venous blood samples were obtained from all patients, and their serum samples were prepared. The levels of serum calcium, β2-MG, and LDH, along with blood hemoglobin and renal functions, were measured. Furthermore, bone marrow samples (3–5 ml/each) were aspirated from nine patients.

Cell lines and cell culture

Human MM ARH-77 cells and human umbilical vein endothelial EA.hy926 cells were purchased from the American

Type Culture Collection (ATCC, Manassas, VA, USA). Human MM RPMI 8226 and U266 cells were obtained from the Shanghai Institute of Cell Biology, Chinese Academy of Science (Shanghai, China). All cells were cultured in Dulbecco's Modified Eagle's Medium supplemented with 10% FBS at 37 °C in a humidified incubator of 5% CO_2.

Isolation of bone marrow plasma cells

Mononuclear cells were isolated from individual bone marrow samples by Ficoll-Hypaque gradient centrifugation. Plasma cells were purified using anti-CD138 microbeads on an AutoMACS system (Miltenyi Biotec, Auburn, CA, USA) following the manufacturer's mannuals.

EVs isolation, purification, and quantification

EVs were isolated by sequential ultracentrifugation. Briefly, individual blood samples were centrifuged at $1000 \times g$ for 30 min. The supernatants were further centrifuged at $13{,}000 \times g$ for 60 min. After being washed with PBS, the pelleted extracellular vesicles were collected after centrifugation at $13{,}000 \times g$ for another 60 min.

Similarly, different groups of MM cells were cultured for 24 h and their cell supernatants were harvested, and then centrifuged at $700 \times g$ for 5 min and $1200 \times g$ for 30 min. Subsequently, the supernatants were subjected to ultracentrifugation as aforementioned to purify EVs. The concentration of EVs were calculated by nanoparticle tracking analysis (NTA) using a Nanosight NS3000 system (Malvern Instruments, United Kingdom) equipped with a 488-nm blue laser. The movement of EVs under Brownian motion was recorded in 10 s sample videos, which were analyzed with NTA analytical software (version 3.2, Nanosight). The pelleted EVs were used for further experiments.

piRNA-823 silencing or upregulation by piRNA-823 inhibitor or mimic treatment

The specific 2'-methoxy-modified RNA oligonucleotides were synthesized and purified by GenePharma (Shanghai, China). has-piRNA-823 mimic was adopted to upregulate endogenous piRNA-823 expression level in the cells, and its sequences were, 5′-AGCGUUGGUGGUAUAGUG GUGAGCAUAGCUGC-3′ (sense); 5′-AGCUAUGCUC ACCACUAUACCACCAACGCUUU-3′ (antisense). has-piRNA-823 mimic non-specific scrambled sequences (mimic-ctrl) were 5′-UUUGUACUACACAAAAGUACU G-3′ (sense); 5′-AAACAUGAUGUGUUUUCAUGAC-3′ (antisense). 1×10^5 EA.hy926 cells were transfected with 100 nM piRNA-823 mimic or 100 nM scrambled control RNA using RiboFECT™ CP Reagent (Ribobio, Guangzhou, China), by following the manufacturer's protocol. has-piRNA-823 inhibitor was designed to suppress endogenous piRNA-823 function and its sequence was 5′-GCAGC UAUGCUCACCACUAUACCACCAACGCU-3′ (sense) and its non-specific scrambled sequence (inhibitor-ctrl) was 5′-AAACAUGAUGUGUUUUCAUGAC-3′ (sense). 2×10^5 RPMI 8226 cells were transfected with 150 nM piRNA-823 inhibitor or 150 nM inhibitor-ctrl as aforementioned. Forty-eight hour later, the transfection efficiency was determined by qPCR.

Analysis of EVs-cells interactions

In order to visualize the transport of piRNA-823 from MM-derived-EVs to ECs, 2×10^5 RPMI 8226 cells were transfected with 100 nM Cy3-labeled piRNA-823 mimic (GenePharma, Shanghai, China). The day after transfection, cells were washed three times with PBS and the medium was changed to fresh DMEM medium. After incubation for 24 h, the culture medium was collected. Then, EVs were isolated and incubated with with CFSE (Sigma-Aldrich, St. Louis, MO, USA) and washed three times by PBS. The transfection efficiency was observed by fluorescence microscope. Then their supernatants were harvested for purification of EVs. Approximately 1×10^8 EVs were incubated with 1×10^5 EA.hy926 cells for 48 h at 37 °C. After washing, the cells were mounted onto slides with mounting medium containing 4', 6-diaminido-2-phenylindole (DAPI; Vector Laboratories, Burlingame, CA, USA). The cells were photoimaged under a confocal laser microscope.

Total RNA extraction and quantitative real-time PCR

Total RNA was extracted from individual EVs or cell samples by employing the TRIzol reagent (Life Technologies, NY, USA). RNA was reversely transcribed into cDNA using the miScript Reverse Transcription Kit (Qiagen, Hiden, Germany) in accordance with the manufacturer's protocol. The relative levels of piRNA-823 to endogenous control RNU6 RNA transcripts were determined by quantitative RT-CR using the miScript SYBR Green PCR Kit (Qiagen, Hiden, Germany) on the Step One Plus Real-Time PCR system (Applied Biosystems, Foster City, CA, USA). The sequences of primers were 5′-AGCGTTGGTGGTA-TAGTGGT-3′ for piRNA-823, 5′-CTCGCTTCGGCAG-CACA-3′ for RNU6F, and 5'-AACGCTTCACGA ATTTGCGT-3' for RNU6R. The RT-PCR was performed in triplicate, and the results were analyzed by $2^{-\Delta\Delta Ct}$.

ECs and MM cell lines co-culture experiments

For transwell co-culture system, ECs were seeded into a 6-well plate, and MM cells were seeded into upper transwell chamber (0.4-μm pore size, Corning Costar, Corning, NY, USA) on another 6-well plate. After 24 h, the media of ECs and MM cells were replaced and MM transwell inserts were moved onto the 6-well plate where ECs were seeded. Twenty-four hour later, the levels of piRNA-823 in ECs were measured by qPCR.

Grouping

We divided ECs into six groups including ECs, ECs^{mimic}, $ECs^{mimic\text{-}ctrl}$, ECs + EVs, ECs + $EVs^{inhibitor}$, and ECs + $EVs^{inhibitor\text{-}ctrl}$ group. Untreated EA.hy926 cells were labeled as ECs group. In ECs^{mimic} group, 100 nM piRNA-823 mimic was transfected into 1×10^5 EA.hy926 cells for 48 h to upregulate piRNA-823 level to directly determine the function of piRNA-823 in ECs. Accordingly, 100 nM piRNA-823 scramble control was transfected into 1×10^5 EA.hy926 cells as negative control and designated as $ECs^{mimic\text{-}ctrl}$ group. To determine the effect of MM-derived-EVs on ECs, 1×10^8 EVs were purified from culture supernatant of untreated MM cells and then incubated with 1×10^5 ECs for 48 h and designated as ECs + EVs group. To further clarify the function of piRNA-823 transferred from MM-derived-EVs into ECs, 150 nM piRNA-823 inhibitor was transfected into 2×10^5 RPMI 8226 cells for 48 h to downregulate the level of piRNA-823 in MM-derived-EVs. Accordingly, these EVs were purified and designated as $EVs^{inhibitor}$. As a control, piRNA-823 scramble control was transfected into MM cells and EVs were designated as $EVs^{inhibitor\text{-}ctrl}$. Then different EVs were incubated with ECs and designated as ECs + $EVs^{inhibitor}$ group or ECs + $EVs^{inhibitor\text{-}ctrl}$ group separately. The differently treated EA.hy926 cells were used for further experiments.

Cell proliferation assay

The proliferation of EA.hy926 cells was determined by CCK-8 assay using the CCK-8 assay kit (DOJINDO, Kumamoto, Japan) by following the manufacturer's instructions.

Transwell invasion assay

The invasion of EA.hy926 cells was determined by transwell invasion assay using 24-well transwell chambers (8-μm pore size, Corning Costar, Corning, NY, USA). 1×10^5 EA.hy926 cells from different groups were added to the upper chamber that had been coated with Matrigel (BD Biosciences, San Jose, CA, USA) and the lower chamber was added with 10% FBS M199 medium. After cultured for 12–24 h, the cells on the top surface of the upper chamber were removed. The invaded cells on the bottom surface of the upper chambers were fixed in 4% paraformaldehyde and stained with crystal violet, and then photoimaged in an inverted phase-contrast microscope. The numbers of cells that penetrated through the membranes on the bottom surface of the upper chambers were calculated at three randomly selected microscopic fields and expressed as fold change relative to the corresponding blank control. Three biological replicates were analyzed using the Student's *t*-test.

Tube formation assay

The tube formation ability of EA.hy926 cells was determined by tube formation assay. Briefly, EA.hy926 cells (2×10^5/well) from different groups were cultured in 24-well plates that had been coated with Matrigel (250 μl/well). The tube formation was examined under a light microscope and the degree of tubulogenesis was quantified by counting branch points. Three biological replicates were analyzed using the Student's *t*-test.

ELISA

The VEGF and IL-6 levels in the supernatants of cultured EA.hy926 cells from different groups were determined by ELISA using the human VEGF and IL-6 ELISA Kits (Neobioscience Technology Co, Beijing, China), respectively, following to the manufacturer's protocol.

Western blot analysis

EA.hy926 cells of different groups were homogenized and lysed. The total proteins (30 μg/lane) were separated by SDS-PAGE and transferred onto PVDF membranes. The membranes were probed with various antibodies, against BCL2, β-Actin, Caspase-3, Cleaved Caspase-3 (Santa Cruz, CA, USA), BAX, GAPDH (Abcam, Cambridge, UK) overnight at 4 °C. After being washed, the blots were incubated with the appropriate horseradish peroxidase-conjugated secondary antibody (Cell Signaling Technology, MA, USA) for 60 min at room temperature. The protein-antibody complexes were visualized using the enhanced chemiluminescent reagent. The relative levels of the target to control protein expression were determined by densitometric scanning using Image J software (Glyko, Novato,CA).

Flow cytometry

Flow cytometry was applied to assess the intracellular ROS and NO levels by using the ROS Assay Kit and fluorescent

probe DAF-FM DA (Beyotime Biotechnology, Shanghai, China), respectively. The single-cell suspension was labeled under specific conditions, and washed twice with PBS. The fluorescent signals were analyzed by flow cytometry using the Flowjo software package.

The EA.hy926 cells of the different groups were stained with a PE-anti-ICAM-1 antibody or PE-anti-CXCR4 antibody (BD Biosciences, San Jose, CA, USA). After being washed, the cells were analyzed by flow cytometry. The percentages of positive cells and their mean fluorescence intensities were measured by using the Flowjo software.

Xenograft murine model

All animal experiments were performed following the recommendations outlined in the policy for Humane Care and Use of Laboratory Animals. The experiment procedures were approved by the Animal Research and Care Committee of Huazhong University of Science and Technology, Wuhan, China.

Female NOD/SCID mice (4–6 weeks of age) were obtained from Beijing HFK Bioscience (Beijing, China). A total of 18 mice were randomly allocated to six groups and were subcutaneously injected with different groups of EA.hy926 cells (5×10^5) mixed with different groups of RPMI 8226 cells (5×10^6) in 100 μl of serum-free media into their right forelimb. The growth and development of tumors were monitored and measured daily using a vernier caliper up for 6 weeks post-injection. A formula of length × width^2 × 0.5 was used to calculate the tumor volumes. At the end of the experiment, the mice were sacrificed, and their tumors were dissected out.

Immunohistochemistry

The levels of CD31, CD34, Ki-67, and Cleaved Caspase-3 in the tumor tissues were immunohistochemically determined by using specific antibodies, including anti-CD31 (Abcam, Cambridge, UK), anti-CD34 (Boster, Wuhan, China), anti-Ki-67, and anti-Cleaved Caspase-3 (Santa Cruz Biotech, CA, USA) by immunohistochemical techniques. The presence of brown staining was considered a positive sign for activated Caspase-3 and Ki-67. Percentages of the positive cells were quantitatively determined by counting 100 cells from three random microscopic fields. A single microvessel was defined as a discrete cluster of cells positive for CD31 or CD34 staining, with no requirement for the presence of a lumen. We quantified the microvessel density (MVD) by selecting three most vascularised areas of the tumour IHC slide and mean values were obtained by counting vessels. The data were analyzed using the Student's *t*-test.

Statistical analysis

Data were expressed as the mean ± SEM. The difference between groups was analyzed by two-tailed student's *t*-test when applicable using Prism GraphPad Software (GraphPad Software, CA, USA). The potential relationship between measurements was analyzed by Spearman's rank correlation coefficient test. A P-value <0.05 was considered statistically significant.

Acknowledgements The authors would like to thank all the participants for their kind cooperation. The research was supported by the National Natural Science Foundation of P.R China (no. 30500686, for Q-LW) and (no. 81770219, for Q-LW).

Compliance with ethical standards

Conflict of interest The authors declare that they have no conflict of interest.

Publisher's note: Springer Nature remains neutral with regard to jurisdictional claims in published maps and institutional affiliations.

References

1. Kyle RA, Rajkumar SV. Multiple myeloma. New Engl J Med. 2004;351:1860–73.
2. Morgan GJ, Walker BA, Davies FE. The genetic architecture of multiple myeloma. Nat Rev Cancer. 2012;12:335–48.
3. Chantrain CF, Feron O, Marbaix E, DeClerck YA. Bone marrow microenvironment and tumor progression. Cancer Microenviron. 2008;1:23–35.
4. Korn C, Mendez-Ferrer S. Myeloid malignancies and the microenvironment. Blood. 2017;129:811–22.
5. Grange C, Bussolati B, Bruno S, Fonsato V, Sapino A, Camussi G. Isolation and characterization of human breast tumor-derived endothelial cells. Oncol Rep. 2006;15:381–6.
6. Hida K, Hida Y, Amin DN, Flint AF, Panigrahy D, Morton CC, et al. Tumor-associated endothelial cells with cytogenetic abnormalities. Cancer Res. 2004;64:8249–55.
7. St Croix B, Rago C, Velculescu V, Traverso G, Romans KE, Montgomery E, et al. Genes expressed in human tumor endothelium. Science. 2000;289:1197–202.
8. Ricci-Vitiani L, Pallini R, Biffoni M, Todaro M, Invernici G, Cenci T, et al. Tumour vascularization via endothelial differentiation of glioblastoma stem-like cells. Nature. 2010;468:824–8.
9. Pezzolo A, Parodi F, Corrias MV, Cinti R, Gambini C, Pistoia V. Tumor origin of endothelial cells in human neuroblastoma. J Clin Oncol. 2007;25:376–83.
10. Streubel B, Chott A, Huber D, Exner M, Jager U, Wagner O, et al. Lymphoma-specific genetic aberrations in microvascular endothelial cells in B-cell lymphomas. New Engl J Med. 2004;351:250–9.
11. Wang R, Chadalavada K, Wilshire J, Kowalik U, Hovinga KE, Geber A, et al. Glioblastoma stem-like cells give rise to tumour endothelium. Nature. 2010;468:829–33.
12. Rigolin GM, Fraulini C, Ciccone M, Mauro E, Bugli AM, De Angeli C, et al. Neoplastic circulating endothelial cells in multiple myeloma with 13q14 deletion. Blood. 2006;107:2531–5.

13. Abdi J, Qiu L, Chang H. Micro-RNAs, New performers in multiple myeloma bone marrow microenvironment. Biomark Res. 2014;2:10
14. Raposo G, Stoorvogel W. Extracellular vesicles: exosomes, microvesicles, and friends. J Cell Biol. 2013;200:373–83.
15. Wang J, Faict S, Maes K, De Bruyne E, Van Valckenborgh E, Schots R, et al. Extracellular vesicle cross-talk in the bone marrow microenvironment: implications in multiple myeloma. Oncotarget. 2016;7:38927–45.
16. Svensson KJ, Belting M. Role of extracellular membrane vesicles in intercellular communication of the tumour microenvironment. Biochem Soc Trans. 2013;41:273–6.
17. Umezu T, Tadokoro H, Azuma K, Yoshizawa S, Ohyashiki K, Ohyashiki JH. Exosomal miR-135b shed from hypoxic multiple myeloma cells enhances angiogenesis by targeting factor-inhibiting HIF-1. Blood. 2014;124:3748–57.
18. Paggetti J, Haderk F, Seiffert M, Janji B, Distler U, Ammerlaan W, et al. Exosomes released by chronic lymphocytic leukemia cells induce the transition of stromal cells into cancer-associated fibroblasts. Blood. 2015;126:1106–17.
19. Canella A, Harshman SW, Radomska HS, Freitas MA, Pichiorri F. The potential diagnostic power of extracellular vesicle analysis for multiple myeloma. Expert Rev Mol Diagn. 2016;16:277–84.
20. Sarkar A, Volff JN, Vaury C. piRNAs and their diverse roles: a transposable element-driven tactic for gene regulation? FASEB J. 2017;31:436–46.
21. Aravin A, Gaidatzis D, Pfeffer S, Lagos-Quintana M, Landgraf P, Iovino N, et al. A novel class of small RNAs bind to MILI protein in mouse testes. Nature. 2006;442:203–7.
22. Girard A, Sachidanandam R, Hannon GJ, Carmell MA. A germline-specific class of small RNAs binds mammalian Piwi proteins. Nature. 2006;442:199–202.
23. Ku HY, Lin H. PIWI proteins and their interactors in piRNA biogenesis, germline development and gene expression. Natl Sci Rev. 2014;1:205–18.
24. Aravin AA, Sachidanandam R, Bourc'his D, Schaefer C, Pezic D, Toth KF, et al. A piRNA pathway primed by individual transposons is linked to de novo DNA methylation in mice. Mol Cell. 2008;31:785–99.
25. Kuramochi-Miyagawa S, Watanabe T, Gotoh K, Totoki Y, Toyoda A, Ikawa M. et al. DNA methylation of retrotransposon genes is regulated by Piwi family members MILI and MIWI2 in murine fetal testes. Genes dev. 2008;22:908–17.
26. Aravin AA, Bourc'his D. Small RNA guides for de novo DNA methylation in mammalian germ cells. Genes Dev. 2008;22:970–5.
27. Cheng J, Deng H, Xiao B, Zhou H, Zhou F, Shen Z, et al. piR-823, a novel non-coding small RNA, demonstrates in vitro and in vivo tumor suppressive activity in human gastric cancer cells. Cancer Lett. 2012;315:12–7.
28. Cui L, Lou Y, Zhang X, Zhou H, Deng H, Song H, et al. Detection of circulating tumor cells in peripheral blood from patients with gastric cancer using piRNAs as markers. Clin Biochem. 2011;44:1050–7.
29. Cheng J, Guo JM, Xiao BX, Miao Y, Jiang Z, Zhou H, et al. piRNA, the new non-coding RNA, is aberrantly expressed in human cancer cells. Clin Chim Acta. 2011;412:1621–5.
30. Yan H, Wu QL, Sun CY, Ai LS, Deng J, Zhang L, et al. piRNA-823 contributes to tumorigenesis by regulating de novo DNA methylation and angiogenesis in multiple myeloma. Leukemia. 2015;29:196–206.
31. Becker A, Thakur BK, Weiss JM, Kim HS, Peinado H, Lyden D. Extracellular vesicles in cancer: cell-to-cell mediators of metastasis. Cancer Cell. 2016;30:836–48.
32. Ogata-Kawata H, Izumiya M, Kurioka D, Honma Y, Yamada Y, Furuta K, et al. Circulating exosomal microRNAs as biomarkers of colon cancer. PloS One. 2014;9:e92921.
33. Manier S, Liu CJ, Avet-Loiseau H, Park J, Shi J, Campigotto F, et al. Prognostic role of circulating exosomal miRNAs in multiple myeloma. Blood. 2017;129:2429–36.
34. Li J, Zhang Y, Liu Y, Dai X, Li W, Cai X, et al. Microvesicle-mediated transfer of microRNA-150 from monocytes to endothelial cells promotes angiogenesis. J Biol Chem. 2013;288:23586–96.
35. Laffont B, Corduan A, Ple H, Duchez AC, Cloutier N, Boilard E, et al. Activated platelets can deliver mRNA regulatory Ago2*-microRNA complexes to endothelial cells via microparticles. Blood. 2013;122:253–61.
36. Umezu T, Ohyashiki K, Kuroda M, Ohyashiki JH. Leukemia cell to endothelial cell communication via exosomal miRNAs. Oncogene. 2013;32:2747–55.
37. Tadokoro H, Umezu T, Ohyashiki K, Hirano T, Ohyashiki JH. Exosomes derived from hypoxic leukemia cells enhance tube formation in endothelial cells. J Biol Chem. 2013;288:34343–51.
38. Skog J, Wurdinger T, van Rijn S, Meijer DH, Gainche L, Sena-Esteves M, et al. Glioblastoma microvesicles transport RNA and proteins that promote tumour growth and provide diagnostic biomarkers. Nat Cell Biol. 2008;10:1470–6.
39. Nazarenko I, Rana S, Baumann A, McAlear J, Hellwig A, Trendelenburg M, et al. Cell surface tetraspanin Tspan8 contributes to molecular pathways of exosome-induced endothelial cell activation. Cancer Res. 2010;70:1668–78.
40. Taverna S, Flugy A, Saieva L, Kohn EC, Santoro A, Meraviglia S, et al. Role of exosomes released by chronic myelogenous leukemia cells in angiogenesis. Int J Cancer. 2012;130:2033–43.
41. Mineo M, Garfield SH, Taverna S, Flugy A, De Leo G, Alessandro R, et al. Exosomes released by K562 chronic myeloid leukemia cells promote angiogenesis in a Src-dependent fashion. Angiogenesis. 2012;15:33–45.
42. Wu Q, Ma Q, Shehadeh LA, Wilson A, Xia L, Yu H, et al. Expression of the Argonaute protein PiwiL2 and piRNAs in adult mouse mesenchymal stem cells. Biochem Biophys Res Commun. 2010;396:915–20.
43. Raaijmakers MH, Mukherjee S, Guo S, Zhang S, Kobayashi T, Schoonmaker JA, et al. Bone progenitor dysfunction induces myelodysplasia and secondary leukaemia. Nature. 2010;464:852–7.
44. Li L, Zhu D, Huang L, Zhang J, Bian Z, Chen X, et al. Argonaute 2 complexes selectively protect the circulating microRNAs in cell-secreted microvesicles. PloS ONE. 2012;7:e46957.
45. Meister G, Landthaler M, Patkaniowska A, Dorsett Y, Teng G, Tuschl T. Human Argonaute2 mediates RNA cleavage targeted by miRNAs and siRNAs. Mol Cell. 2004;15:185–97.
46. Jinek M, Doudna JA. A three-dimensional view of the molecular machinery of RNA interference. Nature. 2009;457:405–12.